Statistical interpretation of topographies and dynamics of multidimensional potentials

Ralph E. Kunz[a)]
Institut für Theoretische Physik, Technische Universität Berlin, Sekr. PN 7-1, Hardenbergstr. 36, D-10623 Berlin, Germany

R. Stephen Berry
Department of Chemistry, The University of Chicago, Chicago, Illinois 60637

(Received 27 January 1995; accepted 27 April 1995)

A statistically based method of characterizing the topography of a multidimensional potential surface classifies not only local minima and saddles but entire basins containing many minima, and divides separating basins and monotonic sequences of local minima within each basin. The data, so classified, fold readily into the formalisms of chemical kinetic isomerization theory and master equations to provide a connection between that topography and the dynamics on the surface. This analysis, in particular, permits an interpretation of the glass-forming or ''focusing'' character of the surface. The method is illustrated with a model system derived, with simplifications, from the 19-atom Lennard-Jones cluster. The method also leads naturally to control problems including the determination of optimum conditions for forming glasses or selected structures, such as particular crystal structures or folded protein structures. © *1995 American Institute of Physics.*

I. INTRODUCTION

Clusters of tens or hundreds of atoms, for the most part, have regular geometries in their low-energy forms, e.g., icosahedral if the interatomic forces are predominantly central and attractive with ranges of ordinary chemical bonds or van der Waals forces, and rocksaltlike if the forces are those of typical ionic salts. However even these simple systems have potential surfaces in their ground electronic states that contain a great many local minima corresponding to amorphous structures. This occurs with rare gas clusters[1] and with alkali halides.[2,3] In the latter study, the $(KCl)_{32}$ cluster exhibited amorphous, locally stable structures outnumbering the rocksaltlike structures by roughly 10^{12}:1. Nevertheless a simulated cluster of $(KCl)_{32}$, initially liquid, whose energy is removed in roughly 25 vibrational periods or more, finds its way to a rocksaltlike structure. Only if the energy is removed in less than about 5 vibrational periods, corresponding to a cooling rate of over 10^{13} K/s, can such clusters fall into the potential wells of amorphous structures.[3,4] This apparent paradox is much akin to the Levinthal paradox in protein structure: the ''wrong'' structures so outnumber the ''correct'' or physiologically active structures of a protein that active proteins and hence organisms could not possibly exist if random search were the mechanism of folding proteins to their active structures. In fact crystal formation by random search is probably more unlikely, statistically, than protein folding, insofar as the constraints on the protein—maintenance of the integrity of the chemical bonds of the polymer chain—rule out many structures that are available to the freely moving atoms on their way to forming a solid.

This example illustrates one pressing issue in the general problem of understanding how the multidimensional potential surfaces of polyatomic molecules, clusters, and nanoscale particles govern the dynamics and phaselike behavior of these systems. It is now practical to explore completely a given potential surface for a system of 8 or perhaps 10 atoms, in the sense of finding all the local minima, all the important saddles linking those minima, and the topology, the connectivity, of all the minima.[5] However, the complexity of potential surfaces increases so rapidly with cluster size that we are most unlikely to wish to create catalogs of all the minima and important saddles for clusters of more than about 15 atoms. For such systems, we need other approaches. We must use statistical samples, not complete data sets, and we need conceptual frames and questions appropriate to such statistical data. Statistical methods have been used before to study complex kinetics[6] but not with the emphasis on the relation between topography and kinetics that is invoked here.

This report presents a way to generate and manipulate such a data set for a many-dimensional potential surface, and to use it to analyze the dynamics on that surface. To illustrate the approach, we have chosen a system of 19 atoms bound by pairwise Lennard-Jones forces. We have made simplifying approximations for expedience and experience, so that our results should be treated as those of a model system, not of a realistic Ar_{19} cluster. Nonetheless, the steps are all clear and without significant difficulties to applying the method in a far more realistic—albeit slower—way.

Our paper is organized as follows: first, in Sec. II, we give a brief introduction to the topic of potential surfaces of clusters and the diagnostic tools used for their exploration. In Sec. III we present our statistical method for the analysis of the topographies of large clusters. Next we estimate the matrix of well-to-well transition rates and incorporate those rates into a master equation governing the dynamics of probability flow within and among basins (Sec. IV). Subsequently, we use the eigenvectors of the master equation to connect the dynamics with the topography of multidimen-

[a)]R.E.K. has also published under the surname ''Breitengraser-Kunz.

 0021-9606/95/103(5)/1904/9/$6.00

sional potential surfaces (Sec. V). Finally we discuss (Sec. VI) and summarize (Sec. VII) our results.

II. POTENTIAL SURFACES OF CLUSTERS

While the potential surfaces of conventional small molecules normally exhibit only one or perhaps a very few stable geometries, clusters of atoms, molecules, or ions, like condensed matter, may be found in any of a large number of locally stable geometric structures. The number of these structures grows extremely rapidly, probably exponentially, with the number of atoms or molecules in the system.[5,7] An important implication is that the study of multidimensional potential surfaces for systems of more than three internal degree of freedom breaks into several categories: at one extreme is the study of systems small enough that it is feasible to catalog all the minima and the important saddles that connect them,[8–10] and to reveal the topography and topology of the surface, both how the geometrically different stable structures are linked and how the geometrically equivalent but permutationally different sets of locally stable structures are connected.[10] Next is the study of potential surfaces that can be modeled and explored fairly extensively so that their densities of locally stable states can be assessed reliably by statistical searches. Finally, there are the forms of bulk matter, for which only the few stable crystalline geometries are relevant to all but amorphous or glassy materials, and for these, sampling can give only a qualitative sense of what kinds of specific geometries may occur, and at best an index parameter of such properties as the extent of long range and short range order.

It is appropriate to point out here that the *topology* of the surface is important insofar as that is what determines the *forms* of the splittings of the quantum states, the splittings that arise from communication among the wells, usually thought of in terms of tunneling but also appropriate for states not very high above the saddles as well. The *topography* of the surface, specifically its quantitative characteristics, determines the *magnitudes* of the various splittings. These complimentary aspects of the potential surfaces will allow us to infer the forms of potential surfaces from high-resolution spectra, as they become available.

Determination of the surfaces is a subject into itself, or really a set of subjects ranging from empirical to *ab initio* generation.[11–19] An aspect of this issue still virtually unexplored but clearly of increasing importance is understanding how well a surface must be known, and whether some kinds of regions need not be known so accurately. Naturally this set of questions is likely to need a context in order to yield any answers: one must ask to what use the surface will be put, in order to know what is meant by ''good enough.'' One tool that will make it possible to carry out such a study systematically is the variation of the topography of a potential by variation of key parameters in the representation of the surface.

Methods for determining minima and saddles have become powerful, efficient, and readily available,[5,7,20–22] provided expressions are available for the potential surfaces. The most important of these are now conjugate gradient,[23] eigenvector following,[7,21,24–29] slowest slides (for saddles),[30–32] and, for Monte Carlo calculations, ''jump-walking.''[33] The recent analysis by Tsai and Jordan explores the accuracy and efficiency of a variety of ways of implementing the eigenvector-following method.[7] One capacity of the search methods that we hope will be used increasingly is the now-demonstrated efficient testing of proposed potential surfaces for their physical plausibility.[31] Since it is now straightforward to find the saddles and minima on a proposed surface for a small polyatomic molecule or cluster, and, thereby, determine whether there are regions of the hypothetical surface that are physically implausible, the user has the opportunity to repair the representation by generating more reliable representations of the regions before using the surface.

The rare gas clusters of 10, 11, 12, and 13 particles all have one kind of deep basin, based on an icosahedral structure, and a relatively large energy gap up to the higher energy structures. Others, such as clusters of 8, 14, and 17 atoms, have far smaller energy gaps between their lowest-energy potential minima and the next local minima, in fact no distinctive energy gaps any place along the energy scale apart from a slightly larger gap at the bottom. The variation from one cluster size to another is an immediate consequence of the particular structures that each size of cluster may exhibit; this kind of variation, highly nonmonotonic with increasing N, indicates that these clusters are all in the regime of small clusters, in Jortner's terms.[34] Larger clusters tend toward monotonic dependence of their properties on N, but even clusters of hundreds of atoms still display some characteristics, such as mean binding energies and dissociation energies for a single atom, that are nonmonotonic, especially when N corresponds to a particular stable closed-shell of ''magic'' number, such as 55, 137, or 309 for Lennard-Jones or Morse clusters, 32 or 250 for binary salts such as NaCl.

Clusters of more than about 15 atoms can be, at present, considered to belong to the second of those categories. They are so complex that we do not want to know all the minima and saddles on their potential surfaces. The Ar_{13} cluster, or at least its Lennard-Jones model, for example, was long thought to have 988 geometrically different minima on its potential surface.[8] However Tsai and Jordan[7] have recently shown that there are 1328, and it is possible that there might be more still, at very high energies. By contrast, they found 464 minima for Ar_{12} (Hoare had found 366), 152 for Ar_{11} compared with Hoare's 145, 64 for Ar_{10} compared with Hoare's 57, and 21 for Ar_9 compared with Hoare's 18. The number of geometrically distinct minima seems to increase at least exponentially with N and the number of permutational isomers of each of those is roughly $N!$.

To develop a way to deal with clusters of $15<N<\sim 10^4$, we chose a system just large enough to require a statistical approach, namely the 19-particle Lennard-Jones cluster. We have made simplifying approximations for expedience and experience, so that our results should be treated as those of a model system, not of a realistic Ar_{19} cluster. Nonetheless, the steps are all clear and without significant difficulties to applying the method in a far more realistic—albeit slower—way.

III. THE METHOD OF TOPOGRAPHY DIAGNOSIS

This section is devoted to the description of a new method to examine topographies of complex potentials and categorize regions of such surfaces into large basins, according to the nature of the structure of the system in the configuration corresponding to the bottom of each basin. We have, for convenience, called the procedure ''topography diagnosis.'' The method is statistical, and carries the study of many-atom systems to the point where one can study dynamics of flows on the surface.

A. Development of the statistical sample

The first phase of our method is generating a statistical data base. We determined a sample of the potential wells visited by the 19-particle Lennard-Jones system with potential energy

$$\phi(\mathbf{r}_1,\ldots,\mathbf{r}_N)=4\epsilon\sum_{i<j}\left[\left(\frac{\sigma}{\mathbf{r}_i-\mathbf{r}_j}\right)^{12}-\left(\frac{\sigma}{\mathbf{r}_i-\mathbf{r}_j}\right)^{6}\right] \tag{1}$$

(where $\epsilon=1.67\times10^{-7}$ J and $\sigma=3.4$ Å are widely used parameters for argon) by quenching at regular intervals[35,36] from high-energy molecular dynamics (MD) runs, carried out with the cluster well in the liquid and thus equipartitioned range of energy. We assume that the system is chaotic and quasiergodic, in the sense that it comes arbitrarily close to every point in the available phase space along its trajectory, and that properties obtained from a time average along the trajectory are the same as those obtained from an ensemble average at an instant, if the ensemble is large enough to correspond to the number of steps along the trajectory. We also determined the saddles linking each successive pair of minima by a hybrid of the eigenvector-following method and the method of slowest slides. Our sample, so determined, consisted of $m=299$ different minima and 461 saddles that linked a pair of minima in the set of 299. The number of geometrically distinct minima on this surface, based on logarithmic extrapolation of the data for Lennard-Jones clusters of 7 through 13 atoms,[7] is probably about half a million. For this reason, we would like to be cautious about the validity of our sample as a representation of the real 19-particle rare gas cluster.

B. Local minima, saddles, and minimum–saddle–minimum connections

The second phase is organization and analysis of these data. The hierarchy of steps in the analysis begins just with listing and ordering the m minima ϕ_j in our sample by energy, i.e., $\phi_j<\phi_{j+1}$ for $j=1,\ldots,m-1$. The most useful organization of the saddles is to catalog them by three numbers, the indices of the two minima that each saddle links and one index for the saddle energy. We chose to order the saddles connecting each pair of minima, e.g., the minima j' and j, according to their potential energy $\phi_{jj'}^{l_{jj'}}$, giving them the index $l_{jj'}$ running from 1 to the number of saddles connecting minimum j' with minimum j. As opposed to systems with few degrees of freedom where the transition between two adjacent wells occurs predominantly via the saddle of lowest energy, many pathways can be used on multidimensional potential surfaces, even pathways with significantly higher energy barriers than that with the lowest barrier. This is possible because the entropic contribution to the transition rates (cf. Sec. IV) may become more important than the energy in determining the mechanism of well-to-well passage, as the particle number and complexity of the surface increase.

The next step of this phase is the compiling and ordering of all the minimum–saddle–minimum (min–sad–min, for convenience) sets $(\phi_{j'},\phi_{jj'}^{l_{jj'}},\phi_j)$. We order these according to the energy of the lower minimum. These triples can be displayed schematically as shown in Fig. 1; this seemingly unintelligible tangle contains all the 461 min–sad–min triples in our sample, plotted with the lower-energy minima on the left-hand side.

From our sample of min–sad–min sets we can address questions of conditional probability. We have computed, for instance, the probability $P(\Delta\phi|\phi_>)$ that the system must cross a barrier with height $\Delta\phi$ to reach a lower minimum conditional on the energy $\phi_>$ of the initial (higher) minimum. Figure 2 shows the mean value and the standard deviation of $\Delta\phi$ in terms of $\phi_>$, with the energies of the $\phi_>$ range partitioned into 9 bins. We find a monotonic increase of the barrier height with decreasing $\phi_>$.

C. Monotonic sequences, basins, and divides

Returning to the triples of the inset of Fig. 1, we see immediately that many of the energies of minima on the right-hand side, the upper minima of each min–sad–min triple, appear also on the left-hand side, as the lower minima of another min–sad–min triple. With the energy resolution of

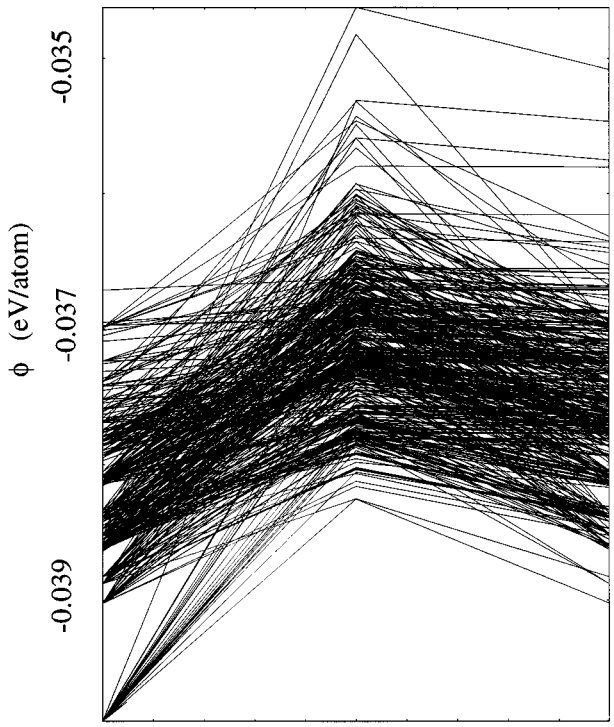

FIG. 1. All minimum–saddle–minimum triples in our data base, gained from MD simulations of Ar_{19}.

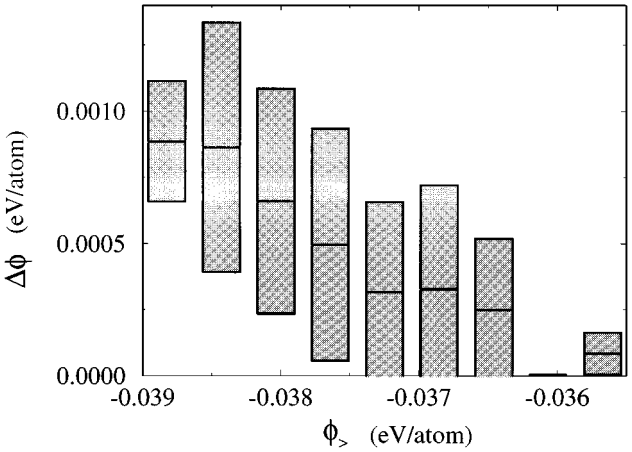

FIG. 2. Mean value and standard deviation of the barrier height $\Delta\phi$ sampled for 9 bins of the energy $\phi_<$ of the initial minimum. The distributions are based on the energy-lowering min–sad–min connections shown in Fig. 1.

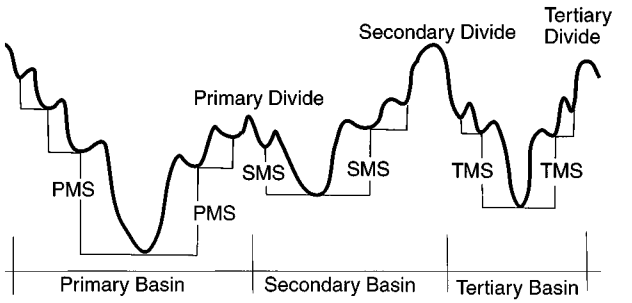

FIG. 3. Schematic representation of primary, secondary and tertiary basins, monotonic sequences, and divides.

our simulation, there are no degeneracies among the minima, apart from permutational isomers; each energy ϕ_j defines a unique, locally stable structure. Hence a minimum at an energy on the left-hand side can be taken as identical with a minimum at the same energy on the right-hand side. This, in turn, means we can unfold the triples into entire sequences of min–sad–min–sad–$\cdots$ points.

The basic ingredients of a classification of entire sequences of pathways turn out to be sequences of local minima with monotonically decreasing energy, or more tersely, *monotonic sequences*. The lower terminus of one or more of such sequences we define as a *basin bottom*, and the local minima lying on them as lying in the corresponding *basin*. The various basin bottoms of a potential surface can then be categorized according to the available structures: into one category, let us say the primary, we can put the global minimum, which has the geometry of the double icosahedron, and any basin bottoms that are only slightly distorted from this reference structure, if such exist. All the monotonic sequences leading to primary basin bottoms we then call *primary* monotonic sequences (PMSs). If a nonprimary monotonic sequence drops down from a minimum on a PMS, we call it a *secondary monotonic sequence* (SMS). We say a basin is a *secondary basin* if the corresponding basin bottom is the lower terminus of at least one SMS. The higher of the two barriers separating the branching minimum from the next lower minima on its two adjacent sequences, one a PMS and the other a SMS, is a *primary divide*. More distant basins, (tertiary, etc.) as well as divides and monotonic sequences are defined analogously. This terminology is illustrated schematically in Fig. 3.

Defining basins based on monotonic sequences of minima is our first working mode of classifying multidimensional potential surfaces. In certain systems such as molecular systems with interactions of strong directionality the role of the divides between different basins may however become more pronounced. In this case we may wish to elaborate the definition when we go to the next stage of including information about the barrier heights.

In our definition we have deliberately not restricted the term ''primary basin'' to the basin containing the global minimum. The reason is not apparent in the example of the Ar_{19} cluster that is our principle vehicle here, but it is in the case of the $(KCl)_{32}$ cluster.[2,3] In that example, it proved useful to distinguish not only the global minimum but all the locally stable forms that have rocksalt structures, even with a few defects. These constitute a class of low-energy forms that define a set of basins that can be classified together as primary. This generalization from a single primary basin for the global minimum to a set of primary basins becomes more and more relevant as the clusters become larger, where interest is in whether the system has found some fcc, hcp, icosahedral, or other type of structure, rather than in whether it has reached the global minimum. Even in the protein folding situation, it is probably useful for purposes of classification to allow systems that have reached a state with the ''right'' physiological activity to have structural differences in irrelevant parts of the system. All such structures can be said to lie in primary basins.

The configurations at the basin bottoms will in general exhibit different patterns of structural order within the cluster evoking the notion of certain phaselike forms, such as, e.g., solid or liquid, but also surface melted,[37,38] core melted,[39,40] or nonwetted,[2,24,41] etc. Hence, using appropriate order parameters a further classification of nonprimary basin bottoms according to phaselike forms seems feasible. This topic will be explored further in the context of dynamic control of phase-like forms in a future publication.

Our sample of Ar_{19} reveals one primary basin, given by the global minimum, and 34 secondary basins. These basins and sequences in our sample are displayed in Figs. 4(a) and 4(b). We find 245 minima on PMSs (a) and 46 on SMSs (b), of which 37 (heavy lines) are connected to a PMS and 9 have ''loose ends'' (thin lines). The primary basin then contains 245, the secondary basins 46 local minima. Eight minima lie on isolated couples, and, amounting to 3% of the overall number, can be seen as the error of our particular statistical survey.

With the aid of the above classification we now have at hand a tool much more powerful for statistical analyses than one based on the min–saddle–min connections alone or even on pair correlations of sequential wells and saddles. To get an overall picture of the barrier heights in the primary basin, we

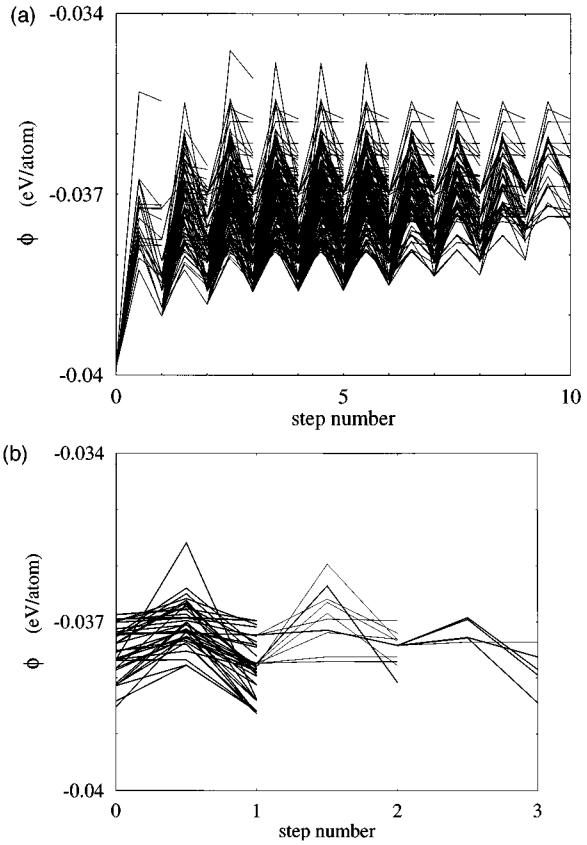

FIG. 4. (a) Primary monotonic sequences (PMSs) in the sample data base for the Lennard-Jones 19-particle cluster; (b) secondary monotonic sequences (SMSs): heavy lines: SMSs connected to a PMS, thin lines: SMSs with loose ends.

computed the distribution of barrier heights as a function of the number of steps to the global minimum on the PMSs of our statistical sample. The average barrier height and the standard deviation in terms of the step number are presented in Fig. 5. We find a slight increase in average barrier height as the system gets closer to the global minimum. In the 19-particle Lennard-Jones system, the saddle energies along the monotonic sequences of minima do not, by any means, form monotonic sequences that parallel the minima; they decrease less rapidly than the minima so that the barrier heights increase slightly, in this system, as the primary basin bottom is approached. We might however suspect both from the finite-time quenching results and from the way we expect nucleation and crystal growth to occur in alkali halides, that for $(KCl)_{32}$ the heights of successive saddles tend to decrease in the direction of the bottoms of the basins corresponding to rocksalt structures.[2,3] This question is under study currently.

IV. MASTER EQUATION DESCRIPTION OF CLUSTER DYNAMICS

This categorization of the surface into basins and wells within them enables us to formulate a simple description for the *dynamics* on a multidimensional potential surface, one that reveals how a system explores configurationally distinct states without having to deal with the complexities of the irregular and, in general, fast, chaotic[42,43] vibrational motion

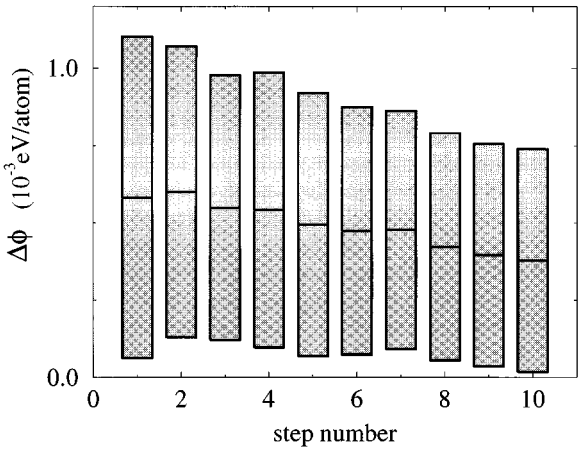

FIG. 5. Mean value and standard deviation of the barrier height $\Delta\phi$ in terms of the downward steps necessary on a PMS to reach the ground basin, based on the PMSs of Fig. 4.

within the wells. Instead, by using transition state theory in any of its forms, we in effect average over these high-frequency modes and concentrate on the slower interwell and interbasin transitions.

A. The thermal transition matrix

There are various methods available to estimate rates for transitions between neighboring potential wells, the choice depending on the accuracy one desires. They range from classical or simple quantum mechanical approaches,[44–46] as given by Rice–Ramsperger–Kassel (RRK) and Rice–Ramsperger–Kassel–Marcus (RRKM) theory, respectively, through phase space approaches,[47,48] to full quantum mechanical S-matrix calculations.[49]

For implementation at the present stage, we have used the RRKM method to estimate interwell transition probabilities. This is a method that gives reliable rates for isomerization of clusters.[50] More elaborate alternative methods are given in Refs. 47 and 48; these will be appropriate to use in the next stages of the method's development. It is now quite feasible to determine the eigenvalues of the Hessian matrix at the minimum of each well, either numerically or analytically,[21,22,29,51] to use those eigenvalues to carry out the RRKM rate calculations in the harmonic approximation[50] and even to include temperature-dependent anharmonic corrections.[2,52]

The derivation of our matrix $\mathsf{W}(T)\equiv[W_{jj'}(T)]_{jj'}$ of transition probabilities, per unit time, at temperature T, from well j' to well j from RRKM theory is performed in the Appendix. It has the form

$$W_{jj'}=\sum_{l_{jj'}} \frac{k_B T}{h}\frac{Q_{jj'}^{l_{jj'}\neq}}{Q_{j'}}\exp(-\Delta\phi_{jj'}^{l_{jj'}}/k_B T), \tag{2}$$

where k_B and h are, respectively, Boltzmann's and Planck's constants, $\Delta\phi_{jj'}^{l_{jj'}}\equiv\phi_{jj'}^{l_{jj'}}-\phi_{j'}$ is the saddle height the system must attain to pass from well j' to well j via saddle denoted $l_{jj'}$, and $Q_{j'}$ and $Q_{jj'}^{l_{jj'}\neq}$ are, respectively, the partition functions of the system in well j' and at the saddle $l_{jj'}$.

The fundamental assumption of transition state theory is the persistence of the system in the region of that saddle long enough for $Q_{jj'}^{l_{jj'}\neq}$ to be well defined. If a harmonic approximation is made for the vibrations, then $Q_{jj'}^{l_{jj'}\neq}/Q_{j'}$ becomes $(h\Pi_{i=1}^{n}\nu_{j',i})/(k_BT\Pi_{i=1}^{n-1}\nu_{jj',i}^{l_{jj'}\neq})$, in terms of $\nu_{j'},i$ and $\nu_{jj',i}^{l_{jj'}\neq}$, the vibrational frequencies or eigenvalues of the Hessian matrices of the j'th well and the corresponding saddle $l_{jj'}$, respectively (cf. Appendix). Here n is the number of the system's vibrational degrees of freedom.

In terms of our description, flows between wells of the same geometry and different permutational order need not be incorporated explicitly into the transition matrix W since dwelling in several permutationally distinct wells is equivalent to staying in one longer. In terms of describing probabilities of different geometries, however, the number of permutational isomers and the connections between them must of course explicitly be taken into account.

B. The master equation

With the matrix W in hand, we can readily construct a linear master equation for the time evolution of the probability distribution $\mathbf{P}(t)\equiv[P_1(t),P_2(t),\ldots,P_m(t)]^T$ in which $P_j(t)$ is the probability that the system be in well j at time t. The equation is

$$\frac{d}{dt}P_j=\sum_{j'=1}^{m} w_{jj'}P_{j'}, \tag{3}$$

where we have let $w_{jj'}\equiv W_{jj'}-\delta_{jj'}\Sigma_{j''}W_{j''j'}$ to simplify the notation. The term for which $j'=j$ corresponds to transitions out of state j, and all other terms, to transitions into state j. For a given potential surface and a fixed temperature each $w_{jj'}$ of the matrix w is constant. Due to $\Sigma_j d/dtP_j=0$, conservation of probability follows from Eq. (3). The structure of the matrix W is that of an adjacency matrix, but the values of the elements are transition rates. The time evolution of $\mathbf{P}(t)$, based on some initial condition $\mathbf{P}(0)$, is the flow of the probability distribution from its initial set of values toward the fully relaxed equilibrium state at that temperature. We assume that the entire phase space of our system is accessible at the high energy of the molecular dynamics simulation, where the cluster is clearly liquidlike, i.e., the energy shell there is compact. This implies that the matrix w is neither decomposable nor splitting, i.e., that it is not, nor can be cast in the form of a block matrix even after possible transient states are erased. In this case there is only one equilibrium state, the Boltzmann distribution $\mathbf{P}^{\mathrm{eq}}$,[53] given by

$$P_j^{\mathrm{eq}}=\frac{Q_j\exp(-\phi_j/k_BT)}{\Sigma_{i=1}^{m}Q_i\exp(-\phi_i/k_BT)}. \tag{4}$$

As a consequence of detailed balance the master Eq. (3) can be symmetrized by introducing a new dependent variable $u_j=P_j/\sqrt{P_j^{\mathrm{eq}}}$.[53] The solution of Eq. (3) can then be expanded in a complete set of eigenvectors $\tilde{\mathbf{u}}^k$ to the symmetric matrix $\tilde{\mathrm{w}}\equiv(\tilde{w}_{jj'})_{jj'}$ with $\tilde{w}_{jj'}=\sqrt{P_{j'}^{\mathrm{eq}}/P_j^{\mathrm{eq}}}w_{jj'}$:

$$P_j(t)=\sqrt{P_j^{\mathrm{eq}}}\sum_{k,k'=1}^{m}\tilde{u}_j^k e^{\lambda_k t}\tilde{u}_{k'}^k\frac{P_{k'}(0)}{\sqrt{P_{k'}^{\mathrm{eq}}}}. \tag{5}$$

The largest eigenvalue of $\tilde{\mathrm{w}}$ is $\lambda_1=0$ corresponding to the equilibrium solution $\tilde{u}_j^1=\sqrt{P_j^{\mathrm{eq}}}$, the other eigenvalues λ_k are negative. The spectral density of fluctuations $S(\omega)$ is

$$S(\omega)=\frac{2}{\pi}\sum_{k=1}^{m}\frac{-\lambda_k}{\lambda_k^2+\omega^2}\left[\sum_{j=1}^{m}\frac{\phi_j\tilde{u}_j^k}{\sqrt{P_j^{\mathrm{eq}}}}\right]^2, \tag{6}$$

which may be possible to relate to spectral line shapes, for eventual comparison of this approach with experiments.

V. CONNECTING TOPOGRAPHY AND DYNAMICS

For a computational illustration of the development presented here, we chose to use an Einstein model for the wells, and assume that they all have the same, single-frequency spectra of intrawell vibrations. The reasons are obviously the ease of doing the calculation, and the unimportance of accurate representation of the real cluster, at this early stage of the development of the method. Since the steps for further refinement are well known, we have simply reserved the execution of computations of a more realistic system for the next stage of the work.

For this test case we constructed the matrix W for our 291-well potential surface, translated, as indicated, to matrix $\tilde{\mathrm{w}}$, and found their eigenvalues and eigenvectors. The individual wells are identified according to basin, i.e., $j\in P$ or $j\in S$ if ϕ_j is in the primary or secondary basin, respectively. They could also be categorized by distance, in a Hamming sense for example,[54] or in the related sense used by Bryngelson and Wolynes,[55,56] from the minimum point of their basin.

Hence the results of this evaluation, apart from yielding the zero-eigenvalue and Boltzmann-distribution eigenvector, show which eigenvectors correspond to intrabasin flows and which to interbasin flows. Moreover the absolute values of the eigenvalues are essentially the inverses of the time constants for these flows. An eigenvector $\tilde{\mathbf{u}}^k$ with nonzero components $\tilde{u}_j^k$ in both primary and secondary basins is associated with flow between these basins. To see whether the *net* flow for that eigenvector is nonzero and into or out of the primary basin, we sum the components of that eigenvector corresponding to wells in the primary basin only. The magnitude of this *net flow index* $f_k=\Sigma_{j\in P}\tilde{u}_j^k\sqrt{P_j^{\mathrm{eq}}}$ determines how important is that flow, and the sign indicates whether flow is into (negative) or out of (positive) the primary basin.

The dark areas in Fig. 6 (right-hand scale) show the distributions of (nonzero) eigenvalues of the master equation, normalized to the Einstein frequency ν_0, for four different temperatures. The entire set of eigenvalues is distributed over seven orders of magnitude at 30 K, over five orders at 60 K, over four at 120, and three at 300 K. Figure 6 also shows the eigenvalues of the eigenvectors dominating the interbasin flows (left-hand scale), corresponding to the 30 largest negative (lightly shaded areas) and positive (solid lines) net flow indices f_k, i.e., flows into and out of the primary basin. These are approximately 100-fold slower than the average of all flows at 30 K, about tenfold slower at 60 K, less than a power of 10 at 120 and indistinguishable at 300 K. Note that these temperatures are simply characteristics of our Einstein model, and not of the real Ar_{19} cluster.

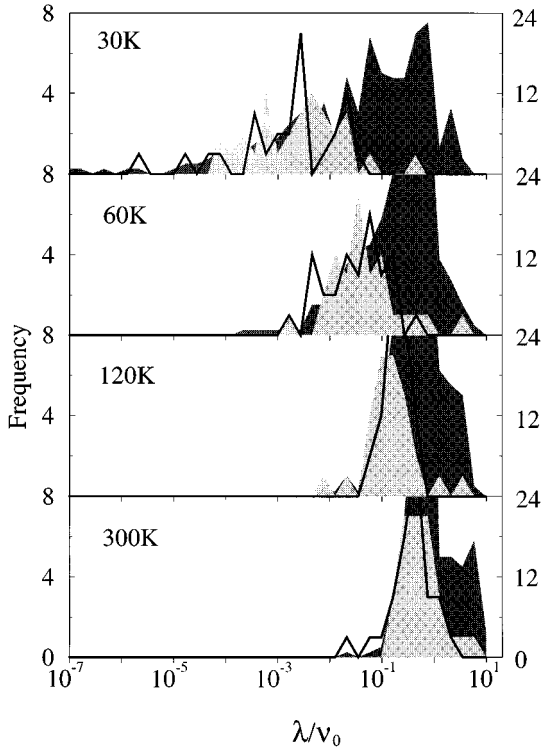

FIG. 6. Binned distributions of eigenvalues of the master equation λ (expressed in terms of the Einstein frequency ν_0) for several temperatures. Areas shaded dark: all nonzero eigenvalues (right-hand scale); light areas and solid lines: 30 eigenvalues with the largest net flow into and out of the primary basin, respectively (left-hand scale).

One can take this analysis one step further, to use the master equation to carry out alternative optimized cooling strategies to bring the system to a preselected mean energy, and thereby to or near a preselected distribution of structures—including, for example, to bring it with high probability to the global minimum, or to a glass. Description of these procedures and their results will be presented in a future report.

VI. DISCUSSION

The analysis presented here, of which preliminary results are contained in Ref. 57 and a short version in Ref. 58, is a first test, based on a relatively small system and a correspondingly small statistical sample, of a new approach to characterize the topography of a multidimensional potential surface and link that topography to the dynamics on the surface. Some of the specific goals have already been described: the conditions for glass transitions and glass formation, and the complementary problem of ''focusing'' surfaces, the evolution of specific kinds of ordered structures and the folding of proteins and other polymers. Others can be enumerated, such as the criteria to determine necessary and sufficient conditions for well-defined phaselike forms to be observable in clusters and nanophase materials, in contrast to gradual transitions from one form to another.

The question arises immediately of the adequacy of the statistical sample. While we have not investigated the adequacy of the sample used here and derived from Ar_{19} we have proposed two criteria of adequacy and are testing those currently. One of these criteria is simply the robustness of the distribution of minima, the density of locally stable states, as a function of energy, to the addition of more minima to the sample, e.g., to doubling the size of the sample set. The other is the robustness of the distribution of monotonic sequences among the various categories of basins, also to the increase in size of the sample set.

More generally, the goal is learning what kinds of information concerning multidimensional potential surfaces are useful. Our own thinking has evolved from studying distributions of minima and saddles to constructing pair correlations, then to devising the concept of, classifying, and scrutinizing entire sequences of minima, and to defining basins and classes of basins. The concept of the class of a basin is still not fully developed, but its main features appear to be clear. For example, all the basins whose minima correspond to structures based on icosahedral geometries and slightly defective versions thereof are presumably all appropriately classed as the same type of basin, at least for large clusters. Close-packed, or perhaps just fcc structures define another type of basin. It is likely that it will be useful to classify bcc and fcc structures as corresponding to different kinds of basins. The categories one wants to use depend, of course, on the nature of the interparticle forces, as illustrated by comparison of the 55-atom Lennard-Jones cluster with the 55-molecule cluster of C_{60}'s. The former has an icosahedral global minimum and a saddle at the cuboctahedral fcc structure, so the latter would be inappropriate as a structure from which to define a type of basin; the latter has a minimum at the cuboctahedron very close in energy to the icosahedral structure.[59] Whether it is useful to say that there are different types of amorphous basins is still one of the open questions.

VII. SUMMARY

We have presented a procedure for studying topography and dynamics on multidimensional potential surfaces. It begins with a descriptive categorization of regions of a given surface, based on the analysis of a statistical sample of saddles and minima on that surface. The special significance of this method is its practicability, as a result of the efficient methods now available for locating minima and saddles on multidimensional potentials. The method then goes on to use transition state theory, at whatever level of accuracy is desired, to compute a matrix of well-to-well transition probabilities, and from this matrix, constructs a master equation whose solutions reveal the intra- and interbasin dynamics of the system moving on this surface.

In addition to work in progress on the reliability of the statistical sample and the basin structure of $(KCl)_{32}$ we are also examining the influence on the glass-forming or focusing character of the surface, of the density of saddles, the distribution of saddle heights along monotonic sequences of minima and the distribution of monotonic sequences among the basins.

ACKNOWLEDGMENTS

R.E.K. thanks Professor E. Schöll and the Deutsche Forschungsgemeinschaft for the opportunity to pursue this work. We would like to thank K.-H. Hoffmann, P. Sibani, and J. C. Schön for fruitful discussions. R.S.B. acknowledges the hospitality of Professor H. Baumgärtel and the Freie Universität Berlin, and the Alexander von Humboldt-Stiftung for its support. We would like to acknowledge Tanya Astakhova's[60] construction of the statistical data base. Support for the study was provided in part by the National Science Foundation.

APPENDIX: RRKM THERMAL TRANSITION RATE CONSTANTS

In general, the calculation of the rate constants requires the knowledge of the intrawell dynamics.[61] However, if the dynamics within the wells occurs on faster time scales than the dynamics among different wells, and the system is quasi-ergodic within the well, the problem can be solved using statistical mechanics. In this Appendix we will use RRKM theory[44] to compute thermal rate constants.

One of the important features of RRKM theory is the use of transition state concepts. They employ the notion of a dividing surface, which separates reactants from products that the trajectory crosses only once. This dividing surface, the transition state, is usually located at the maximum potential energy along the reaction coordinate. Since trajectories only pass through this transition state once, the reaction rate can be obtained by determining the rate at which trajectories cross the dividing surface. The reaction rate is evaluated in terms of the properties of the transition state which is treated thermodynamically even though it is unstable.

From RRKM theory we can easily obtain an expression for the rate constant $K_{j'\to j}^{l_{jj'}}$ for a transition from well j' to j via saddle $l_{jj'}$ at fixed internal energy E:[45]

$$K_{j'\to j}^{l_{jj'}}(E)=\sum_{l_{jj'}} \frac{N_{jj'}^{l_{jj'}\neq}(E)/h}{\rho_{j'}^{v}(E)}. \tag{A1}$$

Here $N_{jj'}^{l_{jj'}\neq}=\int_{\phi_{jj'}^{l_{jj'}}}^{E}\rho_{jj'}^{l_{jj'}\neq}(\epsilon)d\epsilon$ is the sum of vibrational states at the transition state $l_{jj'}$ with potential energy $\phi_{jj'}^{l_{jj'}}$. $\rho_{jj'}^{l_{jj'}\neq}$ and $\rho_{j'}^{v}$ are the densities of vibrational states at the transition state and at the stable configuration, respectively.

Assuming thermal equilibrium at temperature T within the well, the constant energy rate constant $K_{j'\to j}^{l_{jj'}}$ and its thermal analog $k_{j'\to j}^{l_{jj'}}$ are related by[62]

$$k_{j'\to j}^{l_{jj'}}(T)=Q_{j'}^{-1}\int_{\phi_{jj'}^{l_{jj'}}}^{\infty}K_{j'\to j}^{l_{jj'}}(E)\rho(E)\exp(-E/k_BT)dE. \tag{A2}$$

Here $Q_{j'}\equiv\Lambda^{-3n}\int_{\Omega_j'}\exp[-\beta H(\mathbf{q})]d^nq$ is the partition function of the catchment region Ω_j' of minimum j', H is the system's Hamilton function expressed in terms of the canonical coordinates $\mathbf{q}$, $\Lambda=(h^2/2\pi MkT)^{3/2}$, M is the particle mass, and n is the number of the system's vibrational degrees of freedom. We can express $Q_{j'}=\int_{\phi_{j'}}^{\infty}\rho_{j'}(E)\exp(-E/k_BT)dE$ in terms of the density of states $\rho_{j'}$ within $\Omega_{j'}$. Integration in Eq. (A2) begins with energies above the transition state, since $K_{j'\to j}^{l_{jj'}}$ vanishes otherwise. Approximating $\rho_{j'}$ by $\rho_{j'}^{v}$, we obtain Eq. (A3) after integration by parts and substitution of variables

$$k_{j'\to j}^{l_{jj'}}=\frac{k_BT}{h}\frac{Q_{jj'}^{l_{jj'}\neq}}{Q_{j'}}\exp(-\Delta\phi_{jj'}^{l_{jj'}}/k_BT), \tag{A3}$$

where $\Delta\phi_{jj'}^{l_{jj'}}\equiv\phi_{jj'}^{l_{jj'}}-\phi_{j'}$ is the height of the potential barrier for the transition from j' to j and

$$Q_{jj'}^{l_{jj'}\neq}\equiv\int_0^{\infty}\rho_{jj'}^{l_{jj'}\neq}(E)\exp(-E/k_BT)dE \tag{A4}$$

is the partition function at the transition state.

In the harmonic approximation the partition functions $Q_{j'}$ and $Q_{jj'}^{l_{jj'}\neq}$ can be readily computed from the eigenvalues $\nu_{j',i}$ and $\nu_{jj',i}^{l_{jj'}\neq}$, $i=1,\ldots,n$ of the Hessian matrix $(\partial^2\phi/\partial q_j\partial q_{j'})_{jj'}$ at the minimum j' and at the saddle $l_{jj'}$, respectively,

$$Q_{j'}=\prod_{i=1}^{3N-6}(k_BT/h\nu_{j',i}), \tag{A5}$$

$$Q_{jj'}^{l_{jj'}\neq}=\prod_{i=1}^{3N-7}(k_BT/h\nu_{jj',i}^{l_{jj'}\neq}). \tag{A6}$$

Inserting Eqs. (A5) and Eq. (A6) into Eq. (A3) we obtain the final expression for the thermal rate constant in harmonic approximation of RRKM theory:

$$k_{j'\to j}^{l_{jj'}}=\frac{\Pi_{i=1}^{3N-6}\nu_{j',i}}{\Pi_{i=1}^{3N-7}\nu_{jj',i}^{l_{jj'}\neq}}\exp(-\Delta\phi_{jj'}^{l_{jj'}}/k_BT). \tag{A7}$$

We obtain the attempt frequency of the transition as the coefficient to the Arhennius factor, since one vibrational degree of freedom of the transition state has been converted to a translational one and does not enter the denominator of Eq. (A7).

For large enough systems statistical independence of different pathways connecting two given wells can be assumed. We then obtain the probability per unit time for a transition from well j' to well j as

$$W_{jj'}=\sum_{l_{jj'}}k_{j'\to j}^{l_{jj'}}. \tag{A8}$$

[1] A. Rahman, M. J. Mandell, and J. P. McTague, J. Chem. Phys. **64**, 1564 (1976).
[2] J. P. Rose and R. S. Berry, J. Chem. Phys. **98**, 3246 (1993).
[3] J. P. Rose and R. S. Berry, J. Chem. Phys. **98**, 3262 (1993).
[4] H.-P. Cheng and U. Landman, Science **260**, 1304 (1993).
[5] R. S. Berry, Chem. Rev. **93**, 2379 (1993).
[6] J. C. Light, J. Chem. Phys. **40**, 3221 (1988); M. G. Sceats, Adv. Chem. Phys. **70**, 357 (1988); A. Nitzan, *ibid*., p. 489.
[7] C. J. Tsai and K. D. Jordan, J. Phys. Chem. **97**, 11227 (1993).
[8] M. R. Hoare, Adv. Chem. Phys. **40**, 49 (1979).
[9] P. A. Braier, R. S. Berry, and D. J. Wales, J. Chem. Phys. **93**, 8745 (1990).
[10] S. Sawada and S. Sugano, Z. Phys. D **12**, 189 (1989).
[11] J. N. Murell, S. Carter, S. C. Farantos, P. Huxley, and A. J. C. Varandas, *Molecular Potential Energy Functions* (Wiley, New York, 1984).

[12] S. Li, L. Johnson, and J. N. Murell, J. Chem. Soc. Faraday Trans. **88**, 1229 (1992).
[13] J.-Y. Fang, R. L. Johnson, and J. N. Murell, J. Chem. Soc. Faraday Trans. **89**, 1659 (1993).
[14] K. M. Andersson, R. L. Johnston, and J. N. Murell, Phys. Rev. B **49**, 3089 (1994).
[15] D. M. Hirst, *Potential Energy Surfaces* (Taylor and Francis, London, 1985).
[16] D. G. Truhlar, R. Steckler, and M. S. Gordon, Chem. Rev. **87**, 217 (1987).
[17] G. C. Schatz, Rev. Mod. Phys. **61**, 669 (1989).
[18] V. Bonacic-Koutecky, P. Fantucci, and J. Koutecky, Chem. Rev. **91**, 1035 (1991).
[19] J. I. Steinfeld, J. S. Francisco, and W. L. Hase, *Chemical Kinetics and Dynamics* (Prentice–Hall, Englewood Cliffs, 1989), Chap. 7.
[20] R. S. Berry, J. Phys. Chem. **98**, 6910 (1994).
[21] D. J. Wales, J. Chem. Phys. **91**, 7002 (1989).
[22] D. J. Wales, Mol. Phys. **74**, 1 (1991).
[23] W. H. Press, B. P. Flannery, S. A. Teukolsky, and W. T. Vettering, *Numerical Recipes in C*, 2nd ed. (Cambridge University Press, Cambridge, 1992).
[24] J. Pancik, Colloid Czech. Chem. Commun. **40**, 1112 (1975).
[25] R. L. Hilderbrandt, J. Comput. Chem. **1**, 179 (1977).
[26] C. J. Cerjan and W. H. Miller, J. Chem. Phys. **75**, 2800 (1981).
[27] J. Simons, P. Jorgenson, H. Taylor, and J. Ozment, J. Phys. Chem. **87**, 2745 (1983).
[28] A. Banerjee, N. Adams, and J. Simons, J. Phys. Chem. **89**, 52 (1985).
[29] D. J. Wales, J. Chem. Soc. Faraday Trans. **86**, 3505 (1990).
[30] R. S. Berry, H. L. Davis, and T. L. Beck, Chem. Phys. Lett. **147**, 13 (1988).
[31] H. L. Davis, D. J. Wales, and R. S. Berry, J. Chem. Phys. **92**, 4473 (1990).
[32] R. J. Hinde and R. S. Berry, J. Chem. Phys. **99**, 2942 (1993).
[33] D. D. Frantz, J. Chem. Phys. **102**, 3747 (1995).
[34] J. Jortner, D. Scharf, N. Ben-Horin, and U. Even, in *The Chemical Physics of Atomic and Molecular Clusters*, edited by G. Scoles (North-Holland, Amsterdam, 1990).
[35] F. H. Stillinger and T. A. Weber, Phys. Rev. A **25**, 978 (1982).
[36] F. H. Stillinger and T. A. Weber, Kinam 3 Ser. A 159 (1981).
[37] V. V. Nauchitel and A. J. Pertsin, Mol. Phys. **40**, 1341 (1980).
[38] H.-P. Cheng and R. S. Berry, Phys. Rev. A **45**, 7969 (1992).
[39] R. E. Kunz and R. S. Berry, Phys. Rev. Lett. **71**, 3987 (1993).
[40] R. E. Kunz and R. S. Berry, Phys. Rev. E **49**, 1895 (1994).
[41] J. Luo, U. Landman, and J. Jortner, in *Physics and Chemistry of Small Clusters*, edited by P. Jena, B. K. Rao, and S. N. Khanna (Plenum, New York, 1987).
[42] C. Amitrano and R. S. Berry, Phys. Rev. Lett. **6**, 729 (1992).
[43] R. J. Hinde, R. S. Berry, and D. J. Wales, J. Chem. Phys. **96**, 1376 (1992).
[44] J. H. Beynon and J. R. Gilbert, *Application of Transition State Theory to Unimolecular Reactions: An Introduction* (Wiley, Chichester, 1984).
[45] M. F. Jarrold, in *Clusters of Atoms and Molecules*, edited by H. Haberland (Springer, Berlin, 1994), Chap. 2.7.
[46] J. C. Light, Discuss. Faraday Soc. **44**, 14 (1967).
[47] C. E. Klots, J. Phys. Chem. **75**, 1526 (1971).
[48] W. J. Chesnavich, J. Chem. Phys. **66**, 2306 (1977).
[49] M. L. Goldberger and K. M. Watson, *Collision Theory* (Wiley, New York, 1964).
[50] J. P. Rose and R. S. Berry, J. Chem. Phys. **96**, 517 (1992).
[51] D. J. Wales, J. Chem. Soc. Faraday Trans. **89**, 1305 (1993).
[52] F. H. Stillinger and T. A. Weber, J. Chem. Phys. **81**, 5095 (1984).
[53] N. G. van Kampen, *Stochastic Processes in Physics and Chemistry* (North-Holland, Amsterdam, 1981).
[54] R. Hamming, *Coding and Information Theory* (Prentice–Hall, Englewood Cliffs, 1980).
[55] J. D. Bryngelson and P. G. Wolynes, Proc. Natl. Acad. Sci. U.S.A. **84**, 7524 (1987).
[56] J. D. Bryngelson and P. G. Wolynes, Biopolymers **30**, 177 (1990).
[57] R. Breitengraser-Kunz, R. S. Berry, and T. Astakhova, Surf. Rev. Lett. (to be published).
[58] R. S. Berry and R. Breitengraser-Kunz, Phys. Rev. Lett. **74**, 3951 (1995).
[59] D. J. Wales, J. Chem. Soc. Faraday Trans. **90**, 1061 (1994).
[60] Present address: Institute of Chemical Physics, Moscow, 117334, Russia.
[61] P. Hänggi, P. Talkner, and M. Borkovec, Rev. Mod. Phys. **62**, 251 (1990).
[62] R. D. Levine, *Molecular Reaction Dynamics and Chemical Reactivity*, (Oxford University Press, New York, 1987).